FSI TOC

Proceedings of IMECE2002
ASME International Mechanical Engineering Congress & Exposition
November 17–22, 2002, New Orleans, Louisiana

IMECE2002-39025

SELF-EXCITED OSCILLATIONS IN A FLUID-BEAM COLLAPSIBLE CHANNEL

Dr. Z.X. Cai
Department of Mechanics
TianJin University, P.R. China

Dr. X. Y. Luo
Department of Mechanical Engineering
University of Sheffield, Sheffield S1 3JD, UK
E-mail: x.y.luo@shef.ac.uk

ABSTRACT

Unsteady behaviour of a new fluid-beam model for flow in collapsible channels is studied in this paper. A finite element code is developed to solve the fully fluid-structure interaction unsteady problem with method of rotating spines. The self-excited oscillations for different parameters are calculated and compared with these of the earlier fluid-membrane model by Luo & Pedley (1996). A stability line in the tension – wall stiffness space is identified which seems to associate with the small amplitude oscillations which are found only in the new model. As tension is reduced from the stability line, the oscillations undergo a change in amplitude and through to period doubling, highly irregular oscillations with chaotic-like behaviour, and finally divergent. The transition of these different types of oscillations, however, depends on the value of the wall stiffness which is new in this model.

INTRODUCTION

Flow in collapsible tubes has been extensively studied in the recent decades not only due to its relevance to physiological applications, but also because of the interesting fluid-structure interactions that occur. Self-excited oscillations are frequently observed in a Starling resistor made from such a system in the laboratory (Bertram, 1982). Such oscillations have also been obtained from some one-dimensional models, as well as in a two-dimensional fluid-membrane model (Luo & Pedley, 1996) which may, in principle, be realized a laboratory.

The fluid-membrane model, however, suffers from several *ad hoc* approximations: the wall stiffness was ignored, and the elastic wall was assumed to move either in the vertical or in the normal direction. Although these may be adequate for steady flow simulations, their influence on the unsteady flows, especially on the self-excited oscillations, needs to be carefully evaluated. A steady flow study of a new fluid-beam model which employs a plane strained elastic beam with large deflection has been put forward by the authors (Cai & Luo, 2002). In this model the two-dimensional solid mechanics of the wall is taken into account, thus avoiding the above *ad hoc* assumptions. It was found that the steady behaviour of the beam model agrees very well with the membrane model for small values of the wall stiffness.

This paper continues to study on the unsteady flow in the new fluid-beam model, with an aim to identify the possible differences in the self-excited oscillations of the new model and these from the fluid-membrane model by Luo & Pedley (1996).

NOMENCLATURE

A – the cross-sectional area of the beam
c_λ – the dimensionless extensional stiffness of the beam
c_κ – the dimensionless bending stiffness of the beam
D – the undeformed channel height
E – the Young's modulus
F – the force vector in FEM
l – the initial beam position
L – the length of the undeformed beam
L_u – the length of the upstream rigid channel
L_d – the length of the downstream rigid channel
J – bending moment of the beam
K – the nonlinear matrix in FEM
M – the mass matrix in FEM
p – the internal pressure
p_e – the external pressure

Re – the Reynolds number
t – time
T – the longitudinal pre-tension along the beam
u_i (i=1,2) , or u, v– the velocity components
U – the global vector of unknowns in FEM
R – the residual vector in FEM
U_0– the velocity at the inlet
(x,y) - the coordinates
β – the scaling parameter (> 0)
ω – the dimensionless frequency of oscillations
θ– the slope of the deformed beam
λ– the principal stretch of the beam
κ – the curvature of the beam
τ_n – the shear stress of the fluid on the beam
σ – the stress of the fluid
σ_n – the normal stress of the fluid on the beam
ρ – the density of the fluid
ρ_m – the density of the beam
μ – the viscosity of the fluid

A FLUID-BEAM MODEL

The model consists of a flow in a channel in which a part of the upper wall is replaced by an elastic beam, as shown in figure 1.

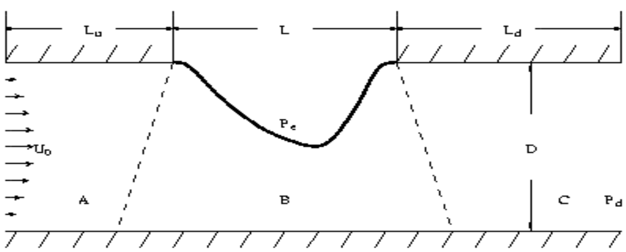

Figure 1: The flow-beam configuration (not to scale). Part B has part of the wall being replaced by an elastic beam.

For convenience, we introduce non-dimensionlized variables as follows:

$$u_i^* = \frac{u_i}{U_0}, \quad \sigma_i^* = \frac{\sigma_i}{\rho U_0^2}, \quad p^* = \frac{p}{\rho U_0^2}, \quad (i = 1, 2)$$

$$T^* = \frac{T}{\rho U_0^2 D}, \; x^* = \frac{x}{D}, \quad y^* = \frac{y}{D},$$

$$t^* = \frac{tU_0}{D}, \; l^* = \frac{l}{D}, \; \kappa^* = \kappa D, \; \rho_m^* = \frac{\rho_m}{\rho D},$$

$$c_\lambda = \frac{EA}{\rho U_0^2 D}, \; c_\kappa = \frac{EJ}{\rho U_0^2 D^3}, \; \mathrm{Re} = \frac{U_0 D \rho}{\mu} \qquad (1)$$

where variables with star are non-dimensional ones which will be used throughout this paper. In the following, however, the stars are dropped for simplicity.

The dimensionless governing equations for the system are thus:

for the beam:

$$\frac{\rho_m}{\lambda}\left(x'\frac{d^2x}{dt^2} + y'\frac{d^2y}{dt^2}\right) = c_\kappa \kappa\kappa' + c_\lambda \lambda' + \lambda\tau_n = 0, \quad \textbf{(2)}$$

$$\frac{\rho_m}{\lambda}\left(y'\frac{d^2x}{dt^2} - x'\frac{d^2y}{dt^2}\right) = c_\kappa\left(\frac{1}{\lambda}\kappa'\right)' - \lambda\kappa T$$
$$-c_\lambda \lambda\kappa(\lambda - 1) - \lambda\sigma_n + \lambda p_e = 0, \quad \textbf{(3)}$$

$$x' = \lambda\cos\theta\,, \qquad (4)$$

$$y' = \lambda\sin\theta\,, \qquad (5)$$

$$\theta' = \lambda\kappa\,. \qquad (6)$$

where the superscript ' denotes differentiation with respect to *l*.

And for the fluid:

$$\frac{\partial u_i}{\partial t} + u_j u_{i,j} = -p_{,i} + \frac{1}{\mathrm{Re}} u_{i,jj}\,, \qquad (7)$$

$$u_{i,i} = 0\,, \quad i, j = 1,2 \qquad (8)$$

where the superscript prime represents derivative with respect to the initial beam position *l*. Notice that as both c_κ and $c_\lambda \to 0$, we recover the fluid-membrane model (Luo & Pedley, 1995).

Boundary conditions for the flow field are chosen such that steady parabolic velocity profile is used for the inlet flow, the stress free condition for the downstream outlet, and the no-slip condition is used along the walls including the elastic section. Clamped conditions are used for the beam ends.

METHOD

A finite element code for unsteady flow is developed to solve the coupled nonlinear fluid-structure interactive equations simultaneously, and an adaptive mesh with rotating spines is used to allow for a movable boundary. The mesh is divided into three subdomains, one of which is placed with many spines originating from the bottom rigid wall to the movable beam, see figure 1.

These spines are straight lines, which can rotate around the fixed nodes at the bottom. Thus all the nodes on the spines can be stretched or compressed depending on the beam deformation. A numerical code is developed to solve the fluid and the beam equations simultaneously using weighted residual methods

A Petro-Galerkin method is used to discretise the system equations (2)-(8). The element type for flow is six-node triangular with second order shape function N_i for u and v, and linear shape function L_i for p. Three-node beam elements with second order shape function are used for x, y, θ, λ and κ. The discretized finite element equations can be written in a matrix form as

$$M(U)\frac{dU}{dt}+K(U)U-F=R=0 \qquad (9)$$

where U $=(u_j,\ v_j,\ p_j,\ x_j,\ y_j,\ \theta_j,\ \lambda_j,\ \kappa_j)$ is the global vector of unknowns, and j=1,…n, is the nodal number. R is the overall residual vector.

An implicit finite difference second order predictor-correct scheme with a variable time step is used to solve the time dependent problem. At each time step, the frontal method and a Newton-Raphson scheme are employed to obtain the converged solution for the whole system simultaneously. In addition, the code is modified to solve the corresponding eigenvalue equations so that the linear stability of the system can be also investigated.

COMPUTATIONAL ACCURACY

The code has been tested for steady flow extensively in terms of grid independence check, as well as comparisons with the analytical solution obtained at the corners of the elastic and rigid walls (Cai & Luo, 2002). In carrying out the numerical calculations, the mesh is chosen such that the boundary layer of a scale $\sqrt{\frac{c_\kappa}{L^2 c_\lambda}}$ can be resolved (Cai & Luo, 2002).

As the time dependent computations are very time consuming, so rather than employing just one (dense) mesh, which can resolve the boundary layers of all the parameters investigated, we choose two different grids. Grid A, a more refined one, which can solve for the smallest value of c_λ (=1) is used for all the simulations with c_λ < 800. In this case, the smallest boundary layer width is estimated to be about 0.0141, and the grid is chosen to be 40 x (60+120+240) with a stretch ratio of 1:10 towards the two corners where the beam joins the rigid wall in both directions. Grid B, the coarser one, where only 18 x (30+60+60) elements are used with the same stretch ratio towards the corners, is used for all the simulations with c_λ >800. In addition, if the amplitude of the oscillations is found to be large, then grid A is always used.

Since variable time steps are used, the temporal accuracy of the solutions are checked by using a different error tolerance ε between $\varepsilon=10^{-5}$ and 10^{-7}. It was found that $\varepsilon=10^{-5}$ is accurate enough for most of the oscillations, see figure 2, with exception for the most violent (chaotic like) ones where small phase difference may occur at the longer time. Since we are not interested in the involutions of the chaotic like oscillations in this paper, $\varepsilon=10^{-5}$ is used throughout the simulations.

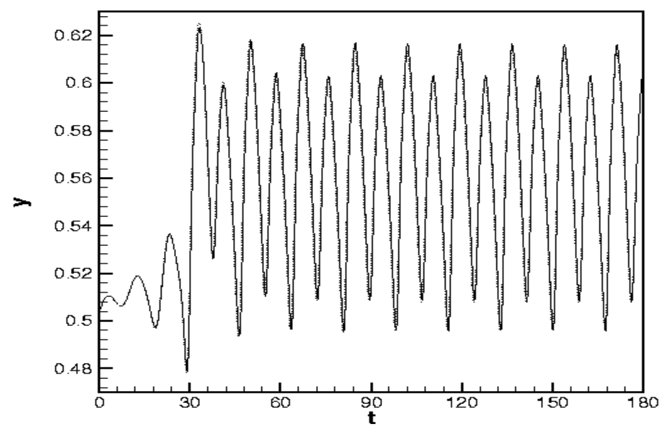

Figure 2. The time dependent position of the wall initially at the beam centre in the y direction for β=30, c_λ=1, Re=300. The solid line indicates the result obtained for $e=10^{-7}$ and the dashed line is for $e= 10^{-7}$.

The computations are performed on a Dec Alpha Unix machine, and take about 0.1-5 CPU minutes for an unsteady solution at any one time step.

RESULTS

Steady solutions:

Steady solutions of the new model have been studied by Cai & Luo (2002); here we only summarize the main results below. All the results are obtained for the following dimensionless parameters:

L_u=5, L=5, L_d=30, D=1,
Re=300, p_e= 1.95, T=178.8/β,
c_κ=10^{-5}-10^{5}, $c_\kappa/c_\lambda=10^{-5}$,

where β is a positive scaling factor for the tension. The ratio of the wall stiffness is chosen to be $c_\kappa / c_\lambda = 10^{-5}$, which is equivalent to choosing the thickness of the wall to be 1% of the channel width.

When c_λ is large, the beam behaves like a rigid wall. The deformation of the elastic wall increases as c_λ decreases. The upstream bulging phenomenon observed in the fluid-membrane model when the tension is below a certain value (Luo & Pedley, 1995) also occurs here when c_λ falls below 100. For c_λ of order unity, this model behaves almost identically to the fluid-membrane model. In other words, the fluid-membrane model seems to be valid for steady flow if c_λ is order 1, see figure 3.

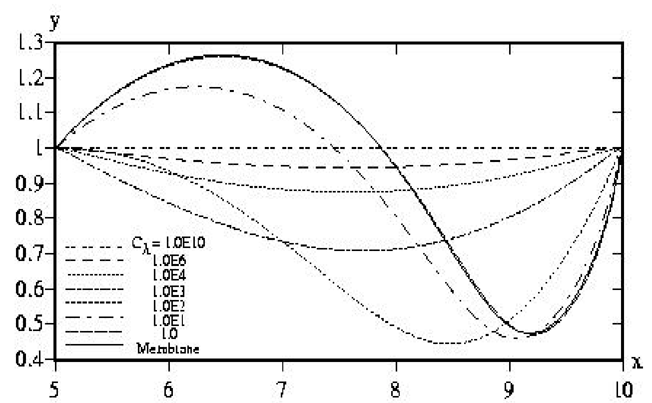

Figure 3: The shapes of the beam for different values of c_λ. Note as $c_\lambda \to 1$, the result agrees closely with the membrane model.

One important difference between the beam and the membrane models is that in the latter, when the tension falls below a critical value (β=181), the numerical scheme breaks down and a steady solution is not attainable (Luo & Pedley, 1995). We found this is only true in the beam model for very small values of c_λ. For c_λ > 1, however, there always exists a finite solution, and the elastic wall approaches to a limiting shape as $T \to 0$. This limiting shape is found to change with the value of c_λ.

Unsteady solutions:

Small perturbations are applied on the steady solutions of the system and the time evolution of the unsteady solutions are subsequently computed. If the perturbations die away as time progresses, then we consider the solutions to be stable.

To check if the unsteady behaviour is similar to that of the membrane model, we start with small wall stiffness, c_λ = 1, where the steady solutions of the two models agree closely with each other. As β is small (tension is big), the solutions in the beam model are found to be stable, see figure 4, below.

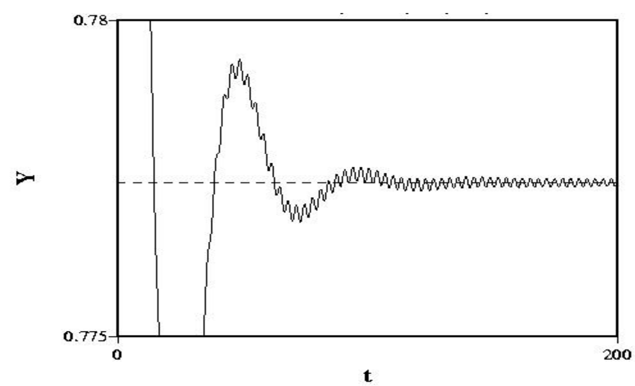

Figure 4. Steady solution obtained for c_λ=1, T=To/β, β=14, is stable to the numerical perturbation. Plotted is the displacement of the initially center point of the beam in y direction , Y, versus time, t.

However, as β is increased (tension is reduced) slightly from 14 to 15, the solution becomes unstable, leading to small amplitude regular waveform oscillations as shown in figure 5. The dimensionless frequency of these kind oscillations is found to be about 1.82. The amplitude of the oscillations for x and y is about 0.00003.

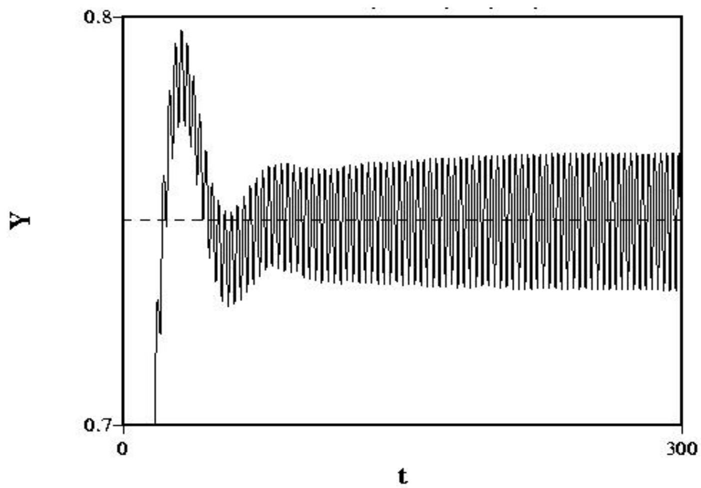

Figure 5. Steady solution obtained for c_λ=1, T=To/β, β=15, is unstable to the numerical perturbation. Plotted is the displacement of the initially center point of the beam in y direction , Y, versus time, t. Small regular sinusoidal amplitude oscillations around their corresponding steady solution (dotted) are developed in time.

Further increase in β, from 15 to 28, gives rise to two remarkable qualitative changes in the oscillations, see figure 6. First, these oscillations become large amplitude with a much lower frequency, of about 0.75 in this case. Secondly, they tend to shift away from the corresponding steady solution. This is different to the small amplitude oscillations.

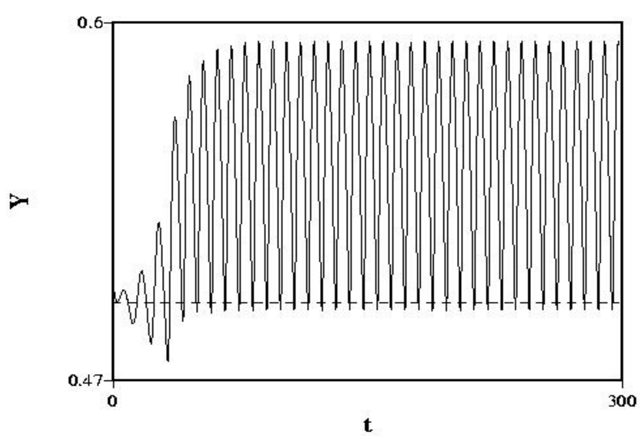

Figure 6. Steady solution obtained for c_λ=1, T=To/β, β=28, is unstable to the numerical perturbation. Large amplitude oscillations are developed in time, they also shifted away from their corresponding steady solution (dotted).

To increase β yet further from 28 to 30, then another distinct phenomenon occurs–period doubling oscillations, see figure 7.

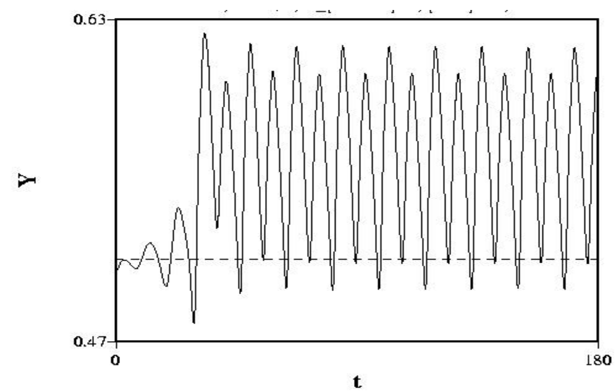

Figure 7. Steady solution obtained for c_λ=1, T=To/β, β=30, is unstable to the numerical perturbation. Large amplitude oscillations are developed in time; the corresponding steady solution is plotted as dotted line. Period doubling is present.

We then increase β still further, from 30 to 35, the period-doubling oscillations are replaced by totally irregular chaotic-like behaviour as shown in figure 8. After this point, any further increase in β will lead to oscillations either too violent for the numerical scheme to cope, or the unsteady solution clearly becomes divergent.

It is noted that the sequence of the unsteady behaviour from figure 4, to figures 6, 7, 8, are qualitatively similar to the unsteady behaviour of the membrane model, in the sense that steady solutions are followed by regular oscillations, then by the period doubling, and finally the chaotic-like oscillations. The differences between the two models for small stiffness (c_λ=1) are that: (a) very few small amplitude oscillations were observed in the membrane model for the parameters studied (Luo & Pedley, 1996), and (b) the values of β for transitions from steady to oscillations, and then period doublings, are slightly different to these of the membrane model (Luo & Pedley, 1996). The latter is understandable, as the tension is a variable in the new model, thus any contributions from the wall stiffness, however small, would alter the real tension in the beam. For the same reason, the frequencies of these large amplitude oscillations (before the period doubling occurs) are also slightly higher than the membrane model for a comparable value of tension (in the new model: ω =0.75, while for the membrane model: ω =0.628).

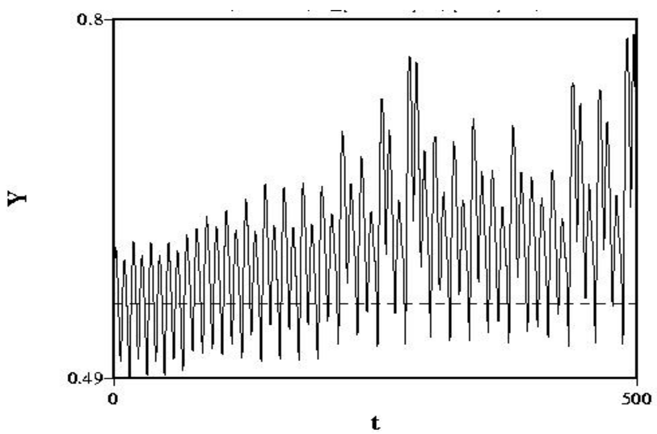

Figure 8. Steady solution obtained for c_λ=1, T=To/β, β=35, is unstable to the numerical perturbation. Large amplitude oscillations are developed in time, the corresponding steady solution is plotted as dotted line. The oscillation is chaotic-like.

These results demonstrated the unsteady behaviour of the beam model for a small value of c_λ. However, it is worth noting that for biological tissues, the values of c_λ ranges between 10^3-10^5 in our dimensionless scale. Therefore, it is important to explore the unsteady behaviour of the beam model for large values of c_λ. For β=33, and c_λ =900, we found that rather than going through the period doubling as shown in figure 6, the oscillation of the system resumes to the small amplitude regular waveform, see figure 9, with almost the same frequency as the one in figure 5 (ω =1.82) !

It is of interests to see if there is a instability pattern in the T-c_λ parameter space. To investigate this, we carried out some considerable computations for the unsteady cases. The preliminary instability pattern is shown in figure 10. It seems that the unsteady solutions are all located under a stability curve in the T- $\boldsymbol{c_\lambda}$ space. Small amplitude oscillations are found to locate on (or just below) the stability curve. The amplitude of these oscillations seems to increase as the solutions move away from the stability curve; the further they are, the more irregular they become.

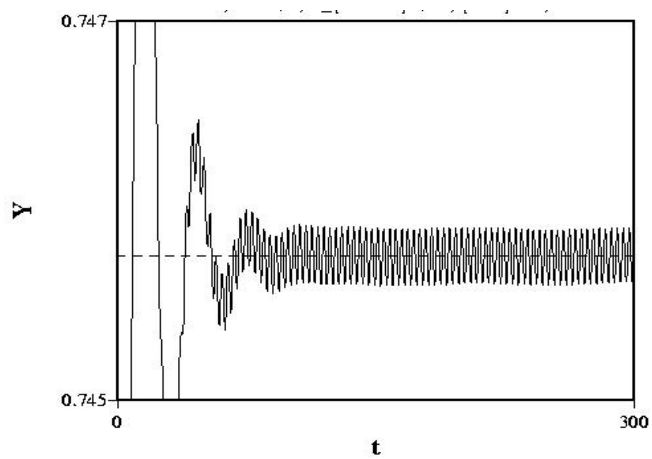

Figure 9. Unsteady solution obtained for c_λ=900, T=To/β, β=33. Small amplitude oscillations are developed in time, the corresponding steady solution is plotted as dotted line.

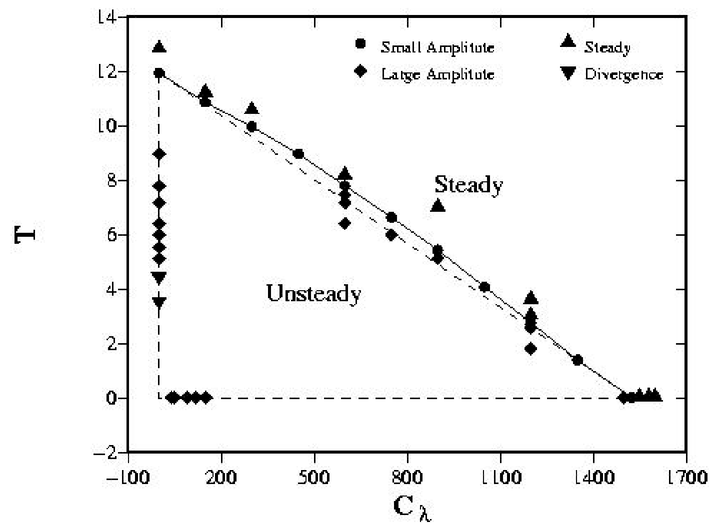

Figure 10 The instability pattern for the beam model as c_λ varies between 1 and 1700. It is seen that the solutions are steady for large values of T and/or c_λ.

DISCUSSION

The results of the new fluid beam model are computed and compared with the fluid-membrane models. There are several interesting discoveries. First, the self-excited oscillations in the new model are qualitatively similar to those from the previous fluid-membrane model if the wall stiffness is very small. This implies that the fluid-membrane model is a good approximation for a very thin wall material (which is usually too thin for biological materials, however). Secondly, small amplitude oscillations are only found so far in the new model with the wall stiffness included.

There seems to exist a stability curve on which the small amplitude oscillations are allocated. It is striking to see that the frequencies of these oscillations are very similar, all within the range of 1.82. These oscillations can then change into the large amplitude irregular non-linear ones via the period doublings as the tension/wall stiffness is further decreased from the stability curve. One finding of interest is that these large amplitude non-linear oscillations tend not to oscillate around their corresponding steady solution when perturbed, but they oscillate around an entirely different operating point. This is a discovery very similar to what has been observed in experiments by Bertram *et al.* (1990), where they found the self-excited oscillations could shift from one steady solution to another one.

It should be mentioned that the parameter study in identifying the stability curve is by no means exhaustive, and the stability curve may or may not be the division of the linear stability of the system. To answer this question stringently, a linear stability study of the eigenvalue problem for the system is required. This is currently being undertaken.

ACKNOWLEDGMENTS

This work is supported by the EPSRC, Grant No. GR/M07243. Special thanks are due to Professor TJ Pedley for his support to this project.

REFERENCES

1. Bertram, C.D. 1982, Two modes of instability in a thick-walled collapsible tube conveying a flow. Journal of Biomechanics, 15, 223-224.
2. Bertram C, Raymond & Pedley TJ, (1990), Mapping of instabilities for flow through collapsed tubes of differing length. *J. of Fluid & Struct.* **369**, 125-153
3. Cai ZX & Luo XY, 2002, A fluid-beam model for flow in collapsible channel, (in press) *J. Fluid & Struct.* 2002
4. Luo XY & Pedley, TJ, 1996, A numerical simulation of unsteady flow in a 2-D collapsible channel, *J. Fluid Mech.* **314**, 191-225.